

PAPER • OPEN ACCESS

Processes controlling the flux of legacy phosphorus to surface waters at the farm scale

To cite this article: Victoria Barcala *et al* 2021 *Environ. Res. Lett.* **16** 015003

View the [article online](#) for updates and enhancements.

ENVIRONMENTAL RESEARCH
LETTERS

LETTER

Processes controlling the flux of legacy phosphorus to surface waters at the farm scale

OPEN ACCESS

RECEIVED

9 September 2020

REVISED

9 November 2020

ACCEPTED FOR PUBLICATION

25 November 2020

PUBLISHED

23 December 2020

Victoria Barcala¹, Joachim Rozemeijer¹, Leonard Osté¹, Bas Van der Griff², Laurens Gerner³ and Thilo Behrends⁴¹ Inland Water Systems, Deltares, Utrecht, The Netherlands² KWR Water Research Institute, Nieuwegein, The Netherlands³ Water Board Rijn and IJssel, Doetinchem, The Netherlands⁴ Department of Earth Sciences, Faculty of Geosciences, Utrecht University, Utrecht, The NetherlandsE-mail: victoria.barcalapaoillo@deltares.nl

Original content from this work may be used under the terms of the [Creative Commons Attribution 4.0 licence](#).

Any further distribution of this work must maintain attribution to the author(s) and the title of the work, journal citation and DOI.



Keywords: legacy phosphorus, leaching, diffuse sources, mitigation measures, groundwater–surface water interactions, agriculture, eutrophication

Supplementary material for this article is available [online](#)**Abstract**

Phosphorus (P) leaching from agriculture is a major driver of water eutrophication in downstream rivers and lakes. In drained lowland areas with intensive agriculture, a reduction in the fertilizer applications may be insufficient to improve the water quality in the short term as the P accumulated in the soil during decades of high fertilization may continue leaching for many years. A complementary approach to reduce P exports from agriculture is to implement edge-of-field mitigation measures at the farm scale. The selection of effective measures requires a detailed insight into the chemical and hydrological transport mechanisms. Here, we determined the main P sources, processes, and transport routes at the farm scale to support the selection of appropriate mitigation measures. We quantified the legacy P, the different P pools stored in the upper soil, and related it to the yearly P export downstream. To do this, we combined high-resolution monitoring data from the soil, groundwater, surface water, and ditch sediments. The legacy P in the topsoil was high, about 2500 kg ha⁻¹. The predominant subsurface flow and the subsoils' P sorption capacity retained the P mobilized from the topsoil and explained the relative moderate flux of P to surface waters (0.04 kg ha⁻¹ during the 2018–2019 drainage season). The dissolved P entering the drainage ditch via groundwater discharge was bound to iron-containing particles formed due to the oxidation of dissolved ferrous iron. Once leached from the soil to the drainage ditch, resuspension of P-rich sediment particles during flow peaks were the most important P transport mechanism (78%). Therefore, we expect that hydraulic constructions that reduce flow velocities and promote sedimentation of P-containing particles could reduce the export of P further downstream.

1. Introduction

Eutrophication of streams and lakes is a global environmental problem; it is triggered by nutrient surplus and causes excessive growth of primary producers such as algae and macrophytes. The European Water Framework Directive obliges member states to achieve a good environmental quality status in streams and lakes. In many inland ecosystems, phosphorus (P) is the nutrient limiting growth (Lee 1973, Dodds and Smith 2016). P can originate from point sources, such as wastewater treatment plants (WWTPs), or diffuse sources, such as runoff or

leaching from agriculture. Point source pollution has been drastically reduced in the last decades with the implementation of P removal in WWTP. Although measures have been taken to restrict P fertilizer applications, agricultural soils maintain a legacy of accumulated P built up after decades of manure and fertilizer application beyond crop requirements. Up to 20 years are needed to confidently detect the water quality improvements caused by changes in agricultural practices (Melland *et al* 2018).

In Europe and other parts of the world, diffuse P is still the most important P source in rivers and lakes (Hart *et al* 2004, Withers and Haygarth 2007). In NW

Europe, agriculture intensified in the decades after the second world war and in recent years P surplus is close to zero (Bol *et al* 2018, McDonald *et al* 2019). The general size and operations of farms in the Netherlands are similar to the ones in other NW European countries (Eurostat 2015). The average farm size in the Netherlands is 29 ha, agriculture is highly intensive, predominantly arable and dairy farming, over flat and artificially drained lands. Around a quarter of the Dutch agricultural land is used in dairy farming, farmers grow grass and maize to feed the cows. Figure 1 shows the P surplus in the Netherlands from 1970 to 2018 (CBS 2020). The livestock production is mainly located in the central, eastern, and southern non-calcareous sandy soils. Historically, most of the manure was applied close to where it was produced (Schoumans 2015). Some of the P surplus remains in the soil as legacy P and can occur structurally bound in minerals, adsorbed to mineral surfaces, or associated with the organic matter present in soil particles. Later, the accumulated P can leach out of the soil with infiltrating rainwater. Therefore, reducing fertilizer or manure applications might not be enough to reduce downstream eutrophication in the short term.

In lowland areas, drainage occurs largely via subsurface flow (groundwater and tube drains) to surface waters (ditches and streams) (Chardon and Schoumans 2007). In Europe, 30 million hectares of agricultural land are artificially drained (Döll and Siebert 2005). Figure 2 shows the share of the arable land that is drained in NW Europe (Brown and Van Beinum 2009), in the Netherlands 60% of the agricultural land is artificially drained. Rozemeijer and Broers (2007) showed that the outflow of drains can contribute up to 80% of the total groundwater-born P flux into surface waters.

Mitigation measures retain P before it is transported downstream and reaches lentic water bodies, which are more prone to become eutrophic. The selection of appropriate measures is not trivial, some make extensive use of arable land, i.e. wetlands and riparian buffers, making their implementation unlikely in areas with high land prices. Other such as water retention measures can increase productivity but may also change the soil moisture and chemical conditions, reducing P sorption and accelerating P transport (Chardon and Schoumans 2007, Schoumans and Chardon 2014). Selecting effective mitigation measures requires detailed insight into chemical and hydrological P transport mechanisms.

In regions with iron-rich groundwater, iron (Fe) is usually reduced and oxidizes as it seeps into the drains or surface waters. During this process, phosphate can be absorbed in Fe-rich colloids or coprecipitate with Fe (hydr)oxides, becoming particulate phosphorus (PP) (Van der Grift *et al* 2014). Fe-bound P can be a significant fraction (38%–95%) of the P in suspended solids in ditches and streams (Van

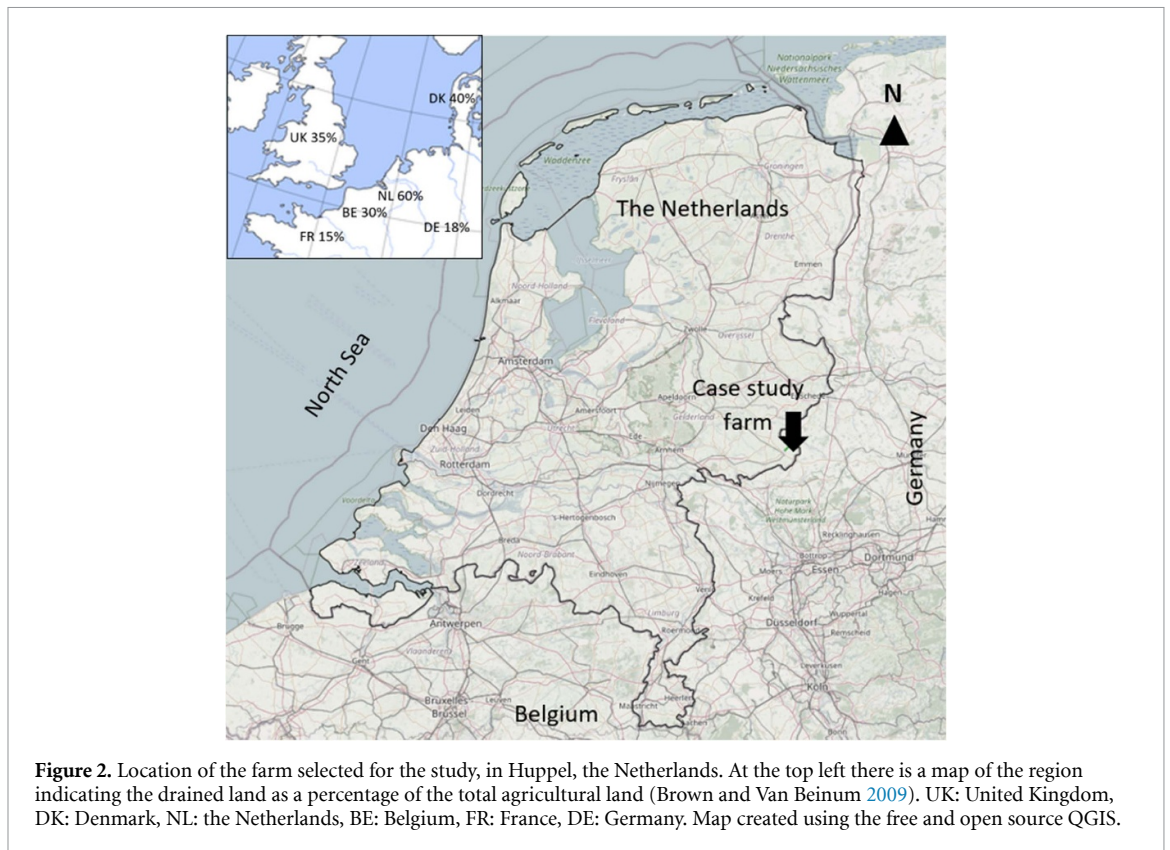
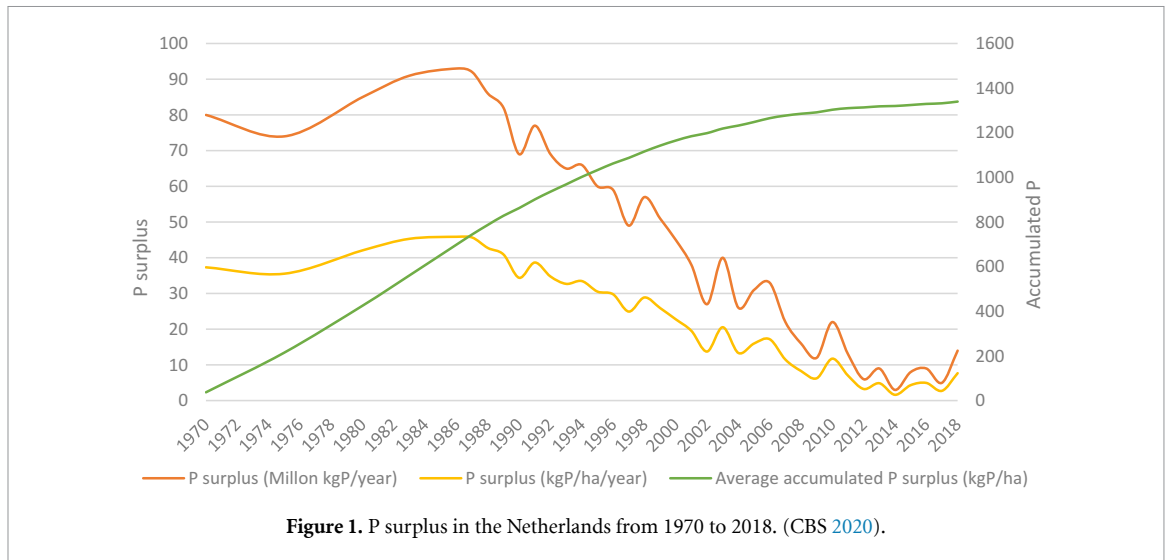
der Grift *et al* 2018). Fe-bound P is less readily available for uptake by algae and less mobile than dissolved phosphate (Baken *et al* 2014). However, once the PP has settled in the sediment, it can be eroded and remobilized during flow peaks, or dissolved under Fe-reducing conditions (Baken *et al* 2015, Mellander *et al* 2016).

Studies on P transport in agricultural landscapes are usually limited to either laboratory or plot scale (Van der Salm *et al* 2011, Van der Grift *et al* 2014), or large catchment scale (De Klein and Koelmans 2011, Baken *et al* 2015, Van der Grift *et al* 2016b). To propose effective mitigation measures there is a need to assess how the known P transport mechanisms aggregate at the farm and small catchment scales, where management interventions are most effective (Bol *et al* 2018). Therefore, the objectives of this study were (a) to identify the main P sources, processes, and transport routes at a farm scale to support the selection of appropriate P retention measures; and (b) to quantify the farm-scale legacy P storage and assess the risk of mobilization and leaching into surface waters.

The study was performed at a farm chosen because of its size and type of production to be representative of drained lowland farms on sandy soils with seasonal manure application in the Netherlands and parts of NW Europe. All the farm water discharges via a single ditch where we placed a high-frequency monitoring station from April 2018 to April 2019. To quantify the P transport routes from the soil to surface water, a water and nutrient balance is presented. Finally, based on these insights, we recommend mitigation measures.

2. Methods

The research site is located in Huppel, the Netherlands, coordinates 52.00131 N, 6.76112 E, 1 km from the Dutch–German border (figure 2). The farm has cows for dairy production and has a size of 24 ha, of which 16 ha are grassland and 8 ha are used for crop farming alternating between corn, beets, and potatoes. A map of the farm is shown in figure 3. Dairy farming has been practiced on the farm since 1930. It can be assumed that the historic agricultural practices on this farm followed the general trend in the Netherlands, where manure application had been intensive until 1989 when a new agricultural policy on fertilizers was introduced. In recent years, the farmer applies an amount of P that will likely be in balance with the crop P uptake, P is added to the soil as manure with injection machinery. The manure is applied early in the season; therefore, the P balance will be known after the crops are harvested. The P surplus considers the actual mass harvested and the P content in the manure for this farm. Thus, the P surplus value fluctuates and some years the balance is positive, and some is negative, but always close to zero in recent years. According to Dutch regulations,



manure can be applied after 1 February on grasslands and from 15 February on arable land, until 1 September. Table 1 presents the P surplus on the farm from 2013 to 2018.

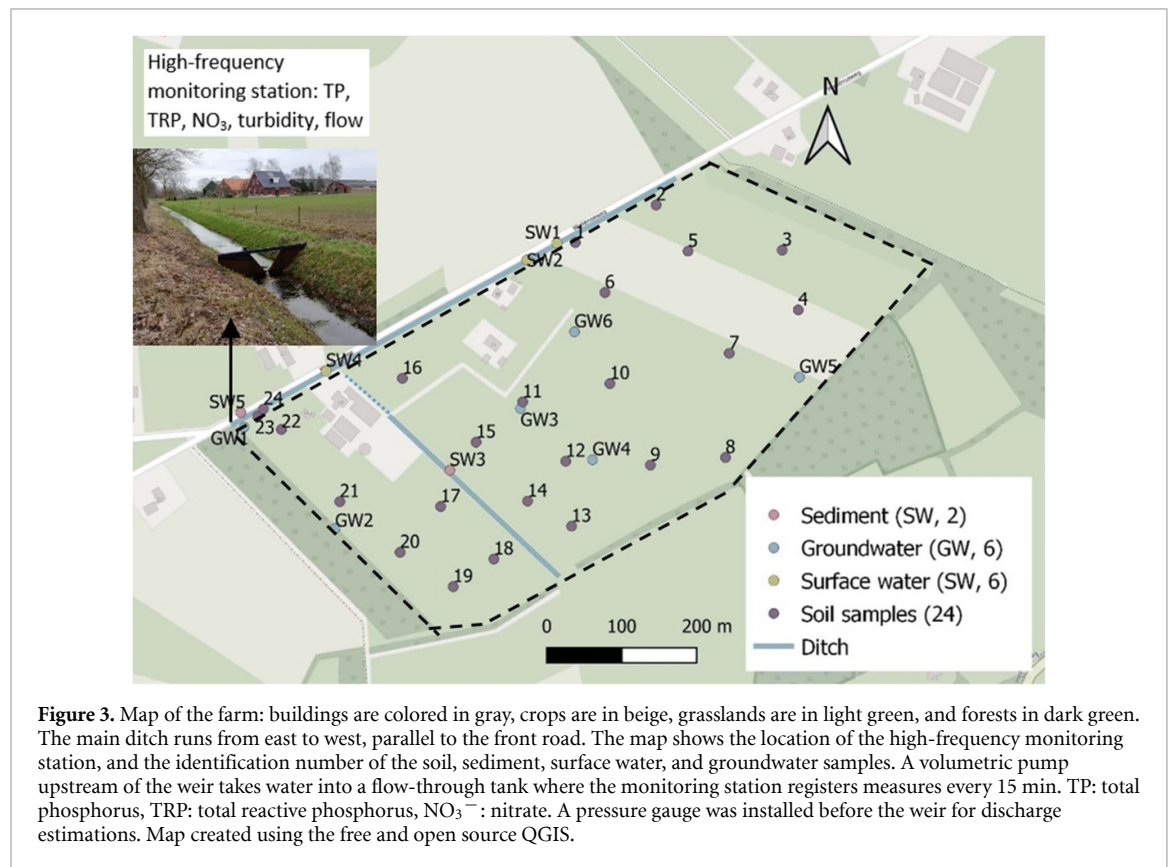
The farm is partly drained with tile drains. The drain tubes are installed at approximately 1 m depth and with 10 m horizontal distance between drains. The altitude is between 35 m and 33.5 m above mean sea level, with a marginal slope directing from east to west. The farm drains to a main ditch that runs from east to west parallel to the front road. The land on the eastern side of the ditch is not connected to the ditch via tile drains and there has been no observations of

surface flow into the ditch originating from land at the eastern side. As infiltrating water in this area discharges into deeper groundwater, it is assumed that the investigated farm is the exclusive catchment area for this ditch. The receiving stream is the Groenlose Slinge, which in summer shows excessive plant growth in front of weirs and blue-green algae blooms in receiving urban canals. The local water authority is considering the implementation of P retention measures in the area.

The farm is located on top of a glacial tunnel valley, which is filled with a fluvioglacial Fe-rich sand layer between 10 m and 20 m deep that lies over

Table 1. P surplus in the farm, as kg P ha⁻¹ the years before the research, from 2013 to 2018.

2013	2014	2015	2016	2017	2018
2 kg ha ⁻¹	-2 kg ha ⁻¹	-6 kg ha ⁻¹	-2 kg ha ⁻¹	1 kg ha ⁻¹	2 kg ha ⁻¹



a marine clay. The combination of sandy soil with the shallow impermeable clay layer makes the system respond relatively quickly to precipitation. More details on the hydrogeology are provided in the supplementary information. The non-calcareous sandy soil present in the farm is characterized by having low levels of P in groundwater (Schoumans and Chardon 2014).

A high-frequency monitoring station (Van der Grift *et al* 2016b) was installed at the westernmost point of the main ditch (figure 3). Just upstream of a V-notch weir, water was pumped to a flow-through vessel where total phosphorus (TP), total reactive phosphorus (TRP), turbidity, and nitrate (NO₃⁻), were registered every 15 min, from 5 April 2018 to 18 April 2019. The discharge was measured by recording water levels upstream of the calibrated V-notch. Table 2 shows an overview of the equipment; more details are provided in the supplementary information.

Soil samples were collected from 24 spots at 0–10 cm and 40–50 cm depth; additionally, four points (4, 10, 14, and 19) were analyzed further at 70–80 cm depth. Sediment samples were also retrieved from the main ditch and a secondary contributing ditch. The soil and ditch sediment samples were taken on 16

April and 15 May 2018, respectively. Soil and sediment samples were stored at 4 °C before being analyzed for soluble P (Pw), labile P (PAL), and TP.

Furthermore, P, Fe, and Al were extracted from soil and sediment samples with ammonium oxalate (Schwertmann 1964). The Fe plus Al obtained from this extraction represents the soil's P sorption capacity, and the molar relation between P and Fe plus Al is the soil's phosphate saturation degree (PSD). The PSD quantifies the P leaching potential (Schoumans and Chardon 2014). In the sediment, the P/Fe ratio from the oxalate extraction quantifies the risk of P mobilization (Smolders *et al* 2017, Van Dael *et al* 2020). Table 3 contains an overview of the soil extraction methods.

Groundwater samples were taken from six monitoring wells at 1.5–2.5 m depth on 15 May 2018 and 18 October 2018. Five surface water samples were taken on 16 April 2018. The water samples were filtered with a 0.45 μm pore size nylon filter and acidified with 1% HNO₃ on-site and analyzed with ICP-OES.

In the period between 20 January and 25 February 2019, the Phosphax auto-analyzer was not working and no TP was measured. To close the gap in the time series TP was estimated using the correlation with NO₃⁻. The precipitation and evaporation

Table 2. Overview of the equipment used in the high-frequency station equipment.

Parameter	Equipment ^a	Method	Detection range	Accuracy ^b
Turbidity	Solitax sensor	Optical (infrared duo scattered light photometer)	0–4000 NTU	1%
NO ₃ [−]	Nitratax sensor	Double wavelength spectrophotometric UV sensor	0.1–50.0 mg l ^{−1}	3%
TRP	Phosphax sigma auto-analyzer	Titration and photometric measurement	0.01–5.00 mg l ^{−1}	2%
TP	Phosphax sigma auto-analyzer	Digestion with H ₂ SO ₄ , titration and photometric measurement (includes mixing and heating/-cooling step)	0.01–5.00 mg l ^{−1}	2%

^aHach Lange GmbH, Düsseldorf, Germany.

^bAccording to the manufacturer.

Table 3. Overview of soil extraction methods used.

Method	Extracting solution	Solution pH	Soil-to-solution ratio	Extraction time	Method of measurement	Elements measured
Pw	Distilled H ₂ O	Unbuffered	1:60	1 h	MBM ^a	P
PAL	Ammonium lactate–acetic acid	3.5	1:20	4 h	MBM ^a	P
Oxalate	Oxalic acid and ammonium oxalate	3	1:50	4 h	ICP-OES ^b	P, Fe, Al
Total ^c	Aqua regia	< 1	3:1	48 h	ICP-OES ^b	P, Fe

^aMolybdenum blue method (MBM) (Murphy and Riley 1962).

^bInductively coupled plasma optical emission spectroscopy (ICP-OES).

^cMore details about the extraction methods are found on the supplement information.

time series from the Hupsel meteorological station, at 12 km distance, were downloaded from the Dutch Royal Meteorological Institute. Additionally, groundwater levels at the farm were continuously monitored with a pressure gauge installed in one well.

3. Results

3.1. Soil, groundwater, and sediment P content

The topsoil consisted of a layer of organic material and roots with high TP and high labile and soluble P and critical PSD. Followed by a layer of brown–red–orange color caused by Fe oxides with no roots and higher P sorption capacity. The underlying sandy layer had a gray–yellow to red–orange color, with little organic matter, and low TP. Figure 4 illustrates how the soil composition, presented in table 4, corresponds to visual appearance. More details on extraction results and pictures from all soil samples are found in the supplementary information.

The average TP content of the soils was 600 mg kg^{−1}, this is high considering previously reported TP contents for non-calcareous sandy soils in the Netherlands which in the range 280–500 mg kg^{−1} (Koopmans *et al* 2006). The average TP concentration in the upper 30 cm of the soil on the farm was 60 200 kg or 2500 kg ha^{−1}, which is higher than the average P in agricultural soils in the Netherlands, 2050 kg P ha^{−1} (Schoumans and Chardon

2014). The total P in the soil accounts for the legacy P plus P in the pre-agricultural soil. The large observed differences between the TP results in the topsoil and subsoil suggested that most of the TP in the topsoil originated from manure and fertilizer application.

In the topsoil, the Pw and PAL values were high, on average 12.2 ± 5.1 mg kg^{−1} and 165.1 ± 68.0 mg kg^{−1} respectively. According to the Dutch Fertilization Grassland and Plants Committee's advice for sandy soils Pw values above 9.8 mg kg^{−1} and PAL values above 109 mg kg^{−1} are high (Commissie Bemesting Grasland en Voedergrassen 2018). Schoumans and Groenendijk (2000) calculated it would take about 30 years for topsoils with Pw of 10 mg kg^{−1} to reach low values (below 4.4 mg kg^{−1}). The Pw results were higher in the arable part of the farm (the northeast side) compared to the grassland part (southwest); PAL and TP show a similar spatial distribution (figure 5). Pw, PAL, and TP notably decrease at 40–50 cm (table 4). Samples 24 and 23 are from both sides of the ditch bank and were not added for the averages in table 4 as they are not representative of the farm's soil. Sample 24 was taken from the between the road and the ditch, which is typically where sediment is laid after dredging the ditch and may explain the high TP concentrations.

In the topsoil, the PSD was 0.26 (table 4). The higher the PSD value, the higher the P saturation in the soil, and the higher the risk of P leaching. The

Table 4. Soil and sediment results: number of samples, averages of Pw, PAL, TP, and oxalate extractions.

Soil samples	<i>n</i>	Pw mg kg ⁻¹ ± SDV mg kg ⁻¹ (as % of TP)	PAL mg kg ⁻¹ ± SDV mg kg ⁻¹ (as % of TP)	TP mg kg ⁻¹ ± SDV mg kg ⁻¹ (as % of TP)	P _{ox} (mmol l ⁻¹)	Fe _{ox} + Al _{ox} (mmol l ⁻¹)	PSD
Depth 0–10 cm	24	12.2 ± 5.1 (2%)	155.1 ± 68.0 (26%)	601 ± 157 (100%)	0.14 ± 0.04	0.50 ± 0.16	0.26 ± 0.07
Depth 40–50 cm	24	1.4 ± 3.53 (1%)	29.5 ± 20.9 (18%)	165 ± 68.3 (100%)	0.03 ± 0.02	0.63 ± 0.38	0.06 ± 0.05
Depth 70–80	4	0.1 ± 0.1 (0.1%)	12.2 ± 6.13 (10%)	113 ± 20.1(100%)	0.01 ± 0.01	0.30 ± 0.18	0.03 ± 0.02
Sediment	<i>n</i>	Pw mg kg ⁻¹ ± SDV mg kg ⁻¹ (as % of TP)	PAL mg kg ⁻¹ ± SDV mg kg ⁻¹ (as % of TP)	TP mg kg ⁻¹ ± SDV mg kg ⁻¹	P _{ox} (mmol l ⁻¹)	Fe _{ox} (mmol l ⁻¹)	P/Fe
Main ditch	2	10.1 ± 0.84 (4%)	41.3 ± 3.2 (17%)	307 ± 92 (100%)	0.04 ± 0.01	0.17 ± 0.01	0.23 ± 0.01
Secondary ditch	1	32 (13%)	108.8 (45%)	241 (100%)	0.08	0.36	0.22



Figure 4. On-site picture of soil sample number 19 (0–100 cm). The topsoil was rich in organic matter followed by a horizon which was brown–red–orange colored due to the presence of iron oxides underlain by a gray–yellow to red–orange sand layer.

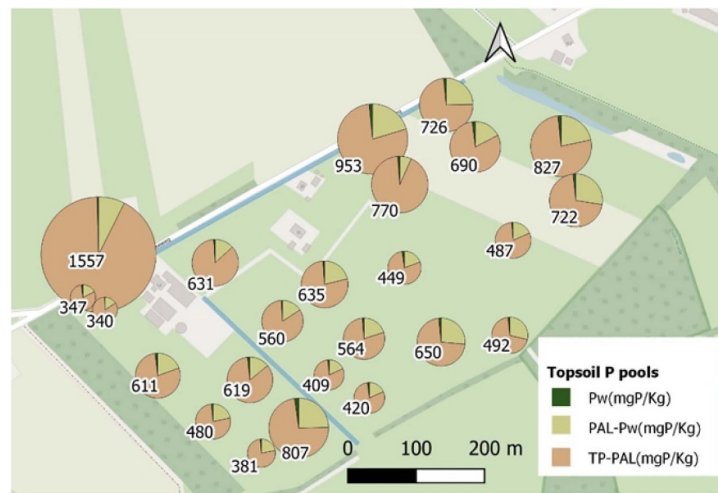


Figure 5. Map showing the total phosphorus contents in the topsoil (0–10 cm) and its distribution over the different sequential extractions at the different sampling locations. The size of the pie charts is proportional to the TP value displayed. Map created using the free and open source QGIS.

critical PSD value for non-calcareous sandy soils is 0.25 (Schoumans and Chardon 2014). In the sediment, the P/Fe ratio was 0.22; critical values for P release from the sediments during summer anoxia are 0.12 for lakes and 0.4 for lowland rivers (Jensen *et al* 1992, Smolders *et al* 2017).

In groundwater the P/Fe molar ratio was calculated for the samples taken on 18 October 2018 (table 5). Some of the P results bear greater uncertainty as they fell below the limit of quantification. Nonetheless, the results show low P concentrations in the groundwater. The Fe concentrations were similar to the average surface water concentrations, $0.21 \pm 0.05 \text{ mg l}^{-1}$.

3.2. Water and solute fluxes

Water and solute fluxes were measured during a very dry year. The precipitation deficit was the highest since the first records in 1957, the accumulated precipitation from April 2018 to April 2019 was 543 mm, while the yearly country average is 800 mm. The

groundwater levels varied between 0.42 m and 1.96 m below surface, with an average of $1.42 \pm 0.42 \text{ m}$. The ditch dried up when groundwater levels fell below 1.20 m; this occurred between 11 May and 22 December 2018.

The water quality parameters measured with the high-frequency sensors showed a distinct behavior depending on the hydrological conditions. To illustrate these different behaviors two periods are shown in detail, a 12 d rainy period and a 4 d dry period. The full-time series from the monitoring station can be found in the supplementary information.

The rain period between 7 January and 18 January 2019 in figure 6 includes hydrological data and data from the high-frequency monitoring station. There were seven subsequent events, with rain intensities between 1 mm h^{-1} and 2 mm h^{-1} , the discharge in the ditch varied from 2 l s^{-1} to about 4 l s^{-1} and the groundwater level fluctuated between 1.1 m and 0.7 m below surface. Turbidity, TP, and TRP peaks occurred simultaneously with a drop in NO_3^- concentration.

Table 5. Groundwater results of dissolved Fe and P concentrations and molar P/Fe.

Groundwater well ^b	15 May 2018	18 October 2018		
	Fe (mg l ⁻¹)	Fe (mg l ⁻¹)	P (mg l ⁻¹) ^a	Molar P/Fe ratio
GW 1	0.767	0.390	0.034	0.16
GW 2	0.011	—	—	—
GW 3	0.011	0.018	0.017	1.8
GW 4	0.107	0.139	0.026	0.29
GW 5	0.302	0.182	0.019	0.19
GW 6	0.033	0.024	0.019	1.4

^aP limit of quantification was 0.026 mg l⁻¹. ^bGW 2 was not sampled on 18 October.

These responses occurred approximately 2 h after the rain peaks. Discharge peaks remobilized P-rich sediment in the ditch as is shown in figure 6 by the simultaneity in the discharge, TP, and turbidity peaks and also by the Fe and P content in the sediment (table 4).

Figure 7 shows the different high-frequency monitored parameters for the selected window with no rain events, from 28 March to 1 April 2019. Especially the TP and TRP and turbidity showed a diurnal fluctuation. This pattern was also detected through the spring of 2018 and 2019, starting in March and continuing until the ditch dried up in April. The highest values for TP, TRP, and turbidity were always measured between 5:00 pm and 7:00 pm and the lowest values around 5:00 am. The groundwater level decreased from 0.88 m up to 0.96 m. The NO₃⁻ concentration fluctuated around 10.5 mg l⁻¹ for the first days and dropped to 9.5 mg l⁻¹.

3.3. Integrated results

Figure 8 shows the cumulative loads for TP and NO₃⁻ during the relatively short drainage season 2018–2019. The total nutrient export for the whole farm over this period was 0.9 kg for P and 282 kg for N. The average TRP was 0.021 mg l⁻¹.

4. Discussion

4.1. Transport of P to the ditch by groundwater flow

A conceptual model of the P fluxes and the water balance for the 2018–2019 drainage season is shown in figure 9. The model includes the main P sources, manure application, and legacy P; the transport processes through the topsoil and subsoil; and finally, the transport and accumulation of P in the ditch. The P concentrations in the soil water from the upper layers were estimated with the correlation between the PSD and the orthophosphate in equilibrium with the soil solution for non-calcareous sand soils found by Schoumans and Groenendijk (2000). When the groundwater levels are high, the water transport through the topsoil carries higher P concentrations. When the water moves through the subsoil layer, the P is adsorbed by the amorphous Fe oxides that have available adsorption sites. This also explains the low dissolved phosphate present in the groundwater

below 150 cm (table 5). The contrast between the TP results in the topsoil and subsoil suggest that most of the TP in the topsoil originated from manure and fertilizer application (table 4).

During the studied drainage period, the water entered the ditch after passing the upper organic-rich layer and the underlying sandy layers of the soil. The dominance of this pathway can be concluded from the similarity of the composition of groundwater and surface water (table S8 (available online at stacks.iop.org/ERL/16/015003/mmedia)); the coupled groundwater level and discharge time series (figures 6 and 7); and no visual observations of overland flow during the 2018–2019 drainage season. This implies that the groundwater level determines the export of dissolved P, which is higher when the infiltrating water does not reach the subsoil with low PSD and unoccupied adsorption capacity and directly discharges into the ditch. At the low groundwater level, there is a net flux from the topsoil into the subsoil and retention of P which reduces the export of dissolved P into the ditch.

In the model the infiltration to deep groundwater was calculated as the difference between the measured precipitation, corrected evapotranspiration, and measured discharge in the ditch; we assume no groundwater storage. The evapotranspiration was obtained using an average crop factor of 0.6 (0.9 for grass and 0.0 for arable land). The infiltration for the period was 89 mm, 2/3 of the precipitation surplus. The presence of the glacial tunnel makes the groundwater flow an important component in the water balance.

4.2. Transport of P in the ditch by remobilization of sediment

The ditch sediment had a different composition of P and Fe pools compared to that of the topsoil (table 4), suggesting the sediment consisted of auto-genic particles and is not formed by eroded topsoil. The sediment's P/Fe ratio and high P_w suggest that P is adsorbed in Fe (oxy)hydroxide colloids, which are important P carriers (Baken *et al* 2016, Van der Grift *et al* 2014, Gu *et al* 2020). The soluble P in the sediment was 0.02 mg l⁻¹ (table S6) which closely matched the TRP baseline in the ditch water (average 0.021 mg l⁻¹), and the soluble P in the sediment (table

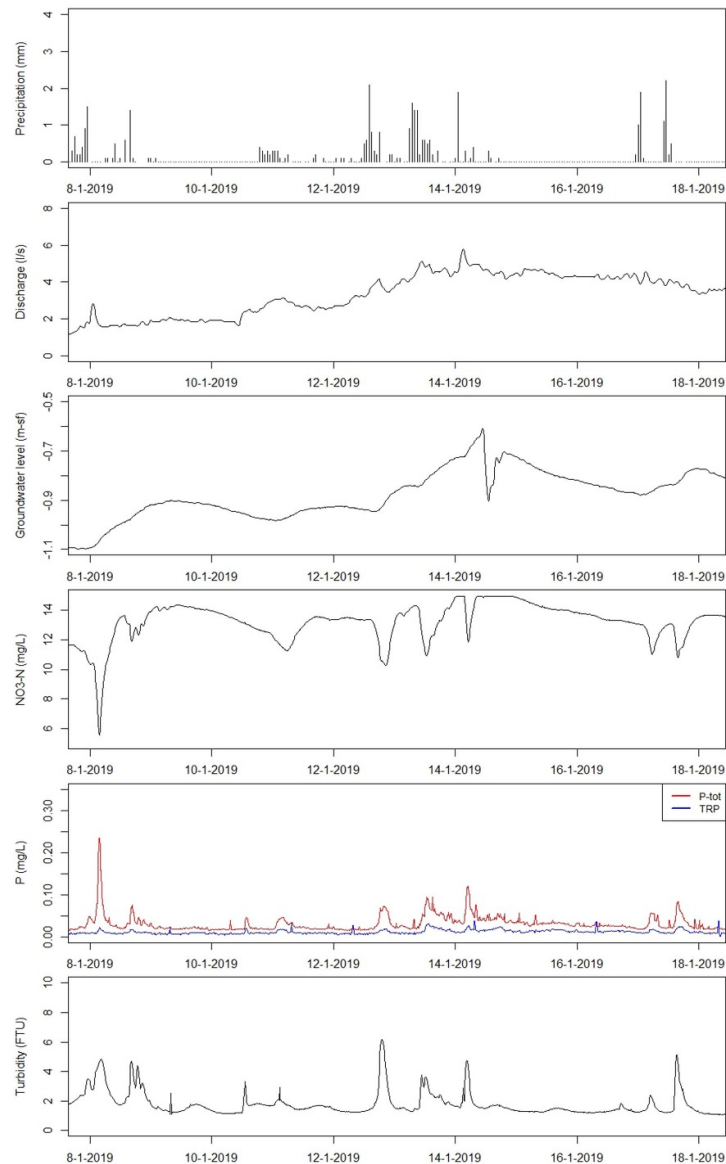


Figure 6. Time series of the precipitation (mm), ditch discharge ($l\ s^{-1}$), groundwater level (meters below ground surface), NO_3^- ($mg\ l^{-1}$), TRP ($mg\ l^{-1}$), TP ($mg\ l^{-1}$) and turbidity (NTU), from 7 January to 18 January 2019.

S6), suggesting the P in the sediment is in equilibrium with the P in the surface water. This implies that during the drainage season the exported TP load consists of 0.20 kg in the form of dissolved P and 0.70 kg in the form of PP, the share of PP in the discharge was 78% of TP, based on the high-frequency monitoring. Nonetheless, the PP fraction of the TP may be even higher, as some Fe-bound P particles are smaller than $0.45\ \mu m$ and may be accounted for in the measurements (Van der Grift *et al* 2016a). TP peaks occurred simultaneously with turbidity after rain events (figure 6). The increase in turbidity is most likely caused by the resuspension of sediments which have freshly deposited in between rain events (figure 10). For the whole period monitored, 76% of TP was exported in 19% of the time when the discharge was above its median, implying that resuspension of PP during high flow events is the major pathway of TP export.

House and Warwick (1998) already reported the importance of particle transport as P carriers during rain events. At a close-by site, Rozemeijer and Van der Velde (2014) recently determined that 60%–90% of the annual P transport was caused by a few rainfall events. De Klein and Koelmans (2011) also found that P transport depended greatly on the seasonal rainfall in the Netherlands.

The TP export per hectare observed in this study was not high, $0.04\ kg\ ha^{-1}$, which can be explained by the vacant sorption capacity of the subsoil. Ulén and Jakobsson (2005) reported a P export of $0.57\ kg\ ha^{-1}\ yr^{-1}$ for a similar catchment in Sweden, a drained agricultural sandy soil with a balanced manure application, but the sand's sorption capacity was low. Gelbrecht *et al* (2005) reported TP exports between $0.04\ kg\ ha^{-1}$ and $0.25\ kg\ ha^{-1}$ for sandy catchments with subsurface flow in NE

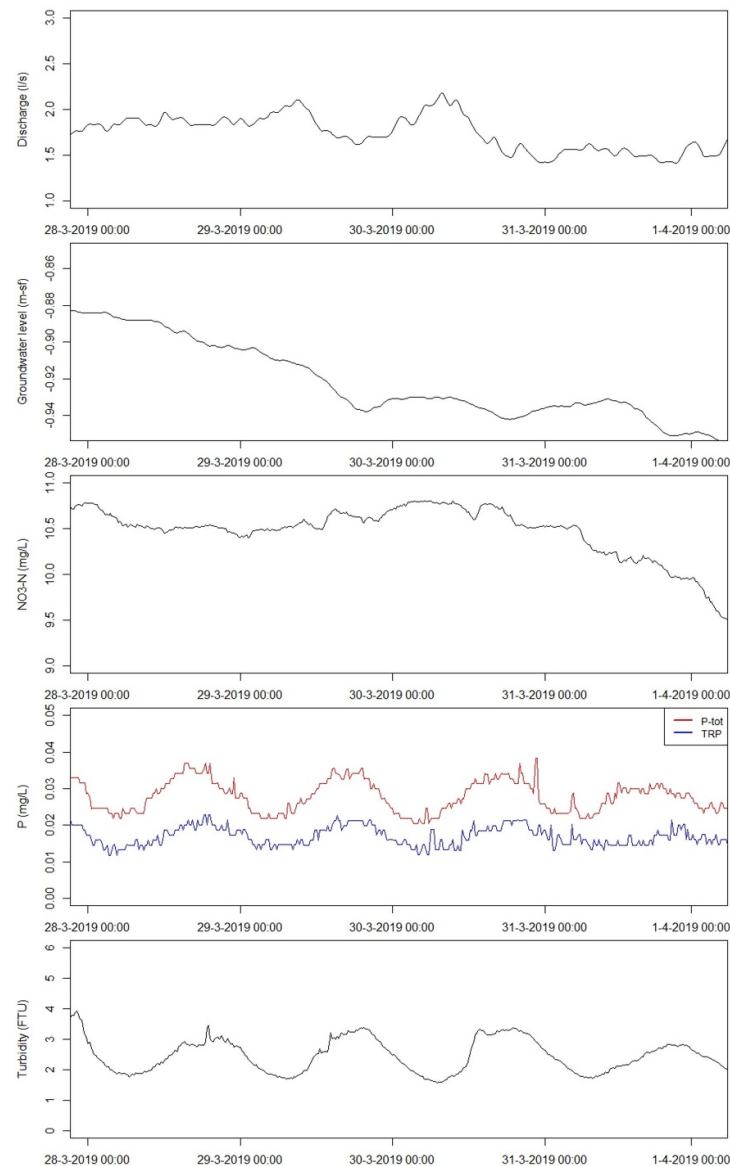


Figure 7. Time series of the ditch discharge (l s^{-1}), groundwater level (meters below ground surface), concentrations of NO_3^- (mg l^{-1}), TRP (mg l^{-1}) and TP (mg l^{-1}), and turbidity (NTU), from 28 March to 1 April 2019.

Germany, however, the sorption capacity of the sand was not reported.

The fact that this was a particularly dry year is one of the main uncertainties to this study, we cannot determine to what extent P retention by subsoil will be as effective in wetter years with higher groundwater levels and even if runoff or soil erosion could occur. Wetter years may result in higher discharge and even higher PP transport downstream. Leaving aside these uncertainties, our results show that PP retention would reduce P losses downstream.

4.3. Phosphorus retention measures

P retention measures, such as sediment traps can reduce the P losses in the short term (Barber and Quinn 2012, Schoumans *et al* 2014). This measure can be implemented alongside water conservation

strategies, which may increase the farmers' willingness to implement them, as water retention offers benefits for the farm during droughts. The measure should buffer the discharge peaks after rain events. This farm has the advantage of having a ditch that catches all the water drained from the farm. The most cost-effective measure should consider this asset, for example by widening the ditch before the weir. Water retention measures were classified as having a very positive impact on PP retention in Swedish sandy lowland areas in the short term (Ulén and Jakobsson 2005). However, not all water retention measures will reduce the yearly P load. First, the outlet should minimize flow peaks and sediment remobilization. For example, some retention water measures widely used in the area include placing inflatable balloons to block culverts. This system only allows open or closed positions causing pronounced transport of

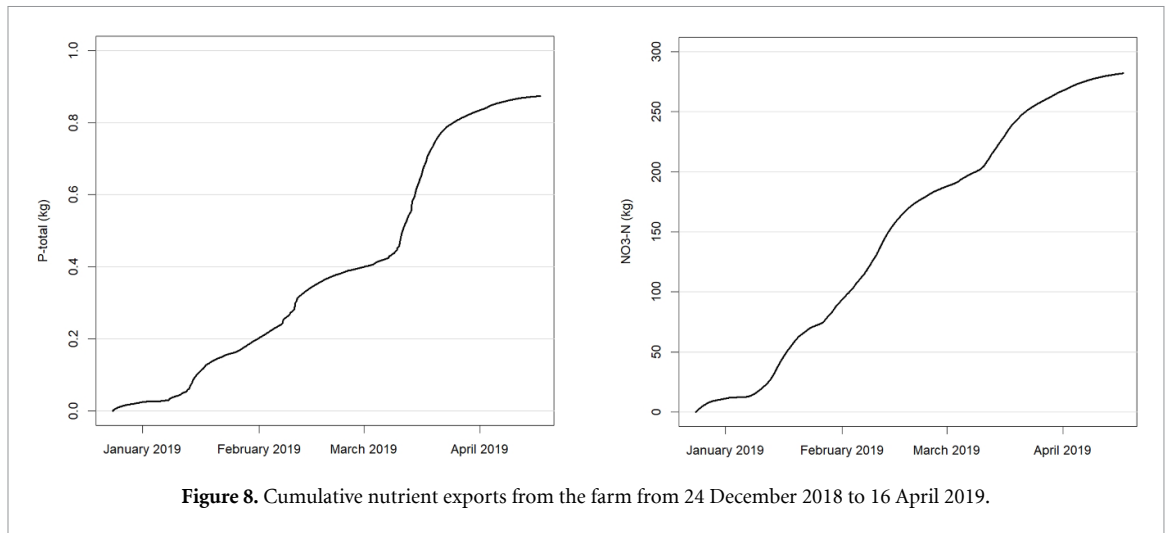


Figure 8. Cumulative nutrient exports from the farm from 24 December 2018 to 16 April 2019.

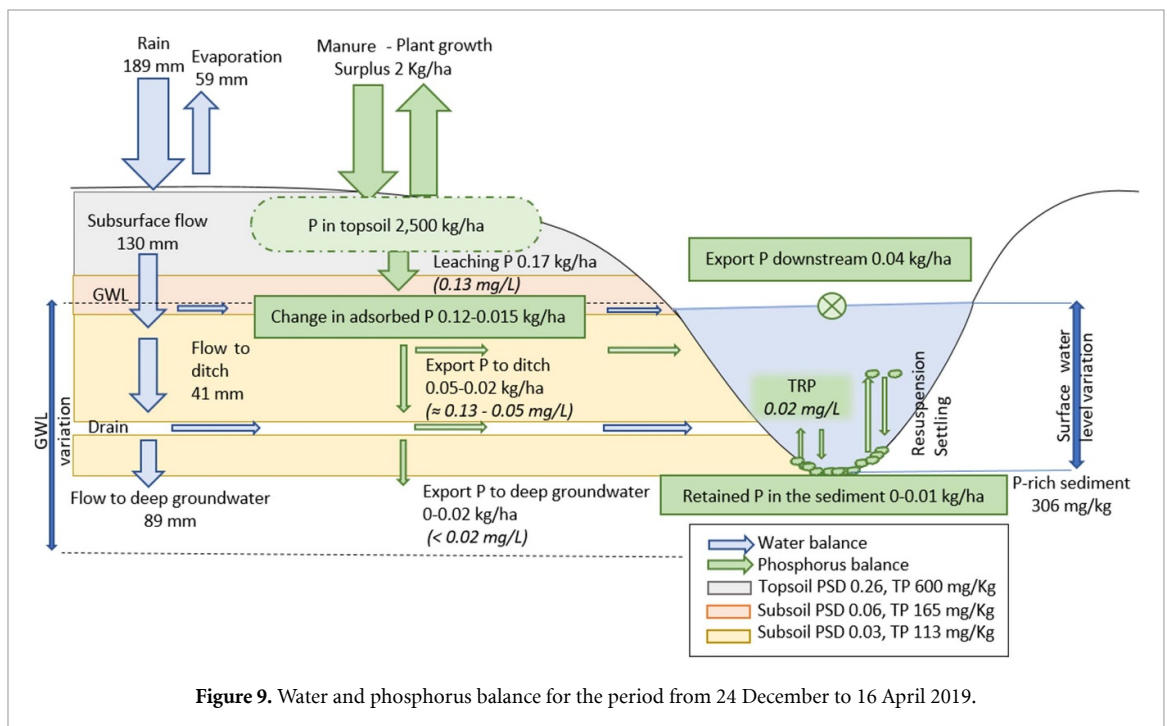


Figure 9. Water and phosphorus balance for the period from 24 December to 16 April 2019.

P-rich sediment when removed. More suitable outlets are adjustable weirs or small diameter pipes. Second, the water retention measure should use the soil's sorption capacity maintaining the groundwater level 40–50 cm below the surface. If the groundwater level was only 20–30 cm below the surface, much more P would reach the ditch as the dissolved P concentrations in the topsoil are higher than in the subsoil due to the saturation of the sorption capacity. Finally, maintenance needs to be considered, removing periodically the sediment from the ditch bottom. From a P recycling perspective, the sediment had a high Pw, which makes it attractive for reuse. Moreover, if the sediments are not removed there is a risk of remobilizing the phosphate present in the sediment once anaerobic conditions are reached.

4.4. Diurnal pattern in phosphorus and turbidity in the spring

Finally, we want to make some remarks on the daily pattern in P concentrations presented in figure 7. The timing of the highest and lowest TP values suggests that the fluctuations are light sensitive, implying that photosynthesis might exert influence on TP concentrations. At the end of March, the solar irradiance goes up at 5 am and reaches zero again around 7 pm. The concentration day vs. night differences are significant ($p < 0.05$), yet the concentration levels are low compared to the water quality target of 0.15 mg l^{-1} . It is relevant that processes other than Fe–P dynamics control the P concentration in surface waters during some part of the year. One hypothesis is that these fluctuations are caused by organisms that sink during nighttime and move to the surface during daytime.



Figure 10. Picture from the main ditch, fluffy orange–red sediments are visible in the bottom.

This was not the first time these daily TP variations are detected. House and Warwick (1998) detected a 30 h variation in TP in April in the River Swale; as levels of dissolved silica also dropped with TP, diatoms were thought to explain the TP variations. Later, Bowes *et al* (2016) detected daily TP variations in the river Thames during the springs of 2009–2013; they observed that most TP fluctuations went in hand with a chlorophyll-*a* increase and phytoplankton growth was associated with the phenomenon. In the same study, another daily TP variation event showed no increase in chlorophyll-*a* but a drop in dissolved silica and diatoms were believed to cause the TP fluctuations. To the best of our knowledge, this daily process has not been thoroughly explained yet. The exact processes and the type of microorganisms that play a role are unknown. In our study area, the TP concentrations during these events are low and do not imply an important P transport year wise.

5. Conclusions

The present study thoroughly followed P from its application until it left the farm through surface water. We investigated the principal P routes in a lowland drained farm on sandy soils, and the findings have implications for similar areas with intensive agriculture. The results show that the topsoil accumulated high amounts of TP with high soluble P concentrations and a critical PSD suggesting a high risk of P leaching. P concentrations in groundwater were low, which could be explained by the dominant

subsurface flow and the unoccupied sorption capacity of the Fe-rich subsoil. In the ditch, most of the exported P was associated to PP resuspension during discharge peaks.

Based on the high proportion of PP and the experiences with trapping P-rich suspended matter (Ulén and Jakobsson 2005, Barber and Quinn 2012), we expect that PP retention could reduce significantly the amount of P leaving the catchment, having a positive impact on downstream eutrophication. Sedimentation traps designed to prevent high discharge peaks are recommended as a suitable P retention measure. We recommend that this approach is used in other areas to identify the main P routes and support the selection of appropriate mitigation measures.

The highlight results of this research are:

- The P in the topsoil, accounted in total 60 200 kg, or 2500 kg ha⁻¹, although nowadays the P input surplus is close to zero, the legacy P is an important component of the P leaving the farm.
- The sorption capacity of the Fe-rich subsoil together with a dominant subsurface flow retained the P and reduced the P losses to surface waters or deeper groundwaters.
- The P export was estimated in total 0.90 kg or 0.04 kg ha⁻¹, for the 2018–2019 drainage season.
- PP transport accounted for 78% of the TP transported downstream, for the 2018–2019 drainage season. Preventing peak flows is important to reduce P-discharge, but also for water retention. We recommend building sediment traps, widening

the ditch or incorporating weirs along the ditch to retain PP.

- The water retention measures implemented should allow the flow to go through the Fe-rich sandy soil.
- In spring TP, TRP, and turbidity showed diurnal fluctuations. This process has been only reported a few times before and might be related to light-sensitive processes as photosynthesis, however, the phenomenon is not yet thoroughly understood.

Data availability statement

All data that support the findings of this study are included within the article (and any supplementary information files).

The data that support the findings of this study are available upon request from the authors.

Acknowledgments

This study was funded by the Province of Gelderland, Water Board Rijn and IJssel, Deltares, and P-TRAP (EU Grant No. 813438, Marie Skłodowska-Curie Actions). We would like to thank farmer Arjan Tolkamp for his cooperation. We would like to acknowledge Edith Eder for her work on this project.

References

- Baken S, Nawara S, Van Moorlegheem C and Smolders E 2014 Iron colloids reduce the bioavailability of phosphorus to the green alga *Raphidocelis subcapitata* *Water Res.* **59** 198–206
- Baken S, Regelink I C, Comans R N J, Smolders E and Koopmans G F 2016 Iron-rich colloids as carriers of phosphorus in streams: a field-flow fractionation study *Water Res.* **99** 83–90
- Baken S, Verbeek M, Verheyen D, Diels J and Smolders E 2015 Phosphorus losses from agricultural land to natural waters are reduced by immobilization in iron-rich sediments of drainage ditches *Water Res.* **71** 160–70
- Barber N J and Quinn P F 2012 Mitigating diffuse water pollution from agriculture using soft-engineered runoff attenuation features *Area* **44** 454–62
- Bol R et al 2018 Challenges of reducing phosphorus based water eutrophication in the agricultural landscapes of Northwest Europe *Front. Mar. Sci.* **5** 1–16
- Bowes M J, Loewenthal M, Read D S, Hutchins M G, Prudhomme C, Armstrong L K, Harman S A, Wickham H D, Gozzard E and Carvalho L 2016 Identifying multiple stressor controls on phytoplankton dynamics in the River Thames (UK) using high-frequency water quality data *Sci. Total Environ.* **569–570** 1489–99
- Brown C D and Van Beinum W 2009 Pesticide transport via sub-surface drains in Europe *Environ. Pollut.* **157** 3314–24
- CBS 2020 Mineral balance agriculture (available at: opendata.cbs.nl/statline/#/CBS/nl/dataset/83475NED/table?=&1601641484793) (Accessed 6 January 2020)
- Chardon W J and Schoumans O F 2007 Soil texture effects on the transport of phosphorus from agricultural land in river deltas of Northern Belgium, The Netherlands and North-West Germany *Soil Use Manage.* **23** 16–24
- Commissie Bemesting Grasland en Voedergewassen 2018 Bemestingsadvies (available at: <https://edepot.wur.nl/413891>)
- De Klein J J M and Koelmans A A 2011 Quantifying seasonal export and retention of nutrients in West European lowland rivers at catchment scale *Hydrol. Process.* **25** 2102–11
- Dodds W K and Smith V H 2016 Nitrogen, phosphorus, and eutrophication in streams *Inland Waters* **6** 155–64
- Döll P and Siebert S 2005 A digital global map of artificially drained agricultural areas *Frankfurt Hydrology Paper 04* (Institute of physical geography, Frankfurt University) (Issue 01) (<https://doi.org/10.13140/2.1.3971.3923>)
- Eurostat 2015 Farm structure survey (available at: <https://ec.europa.eu/eurostat/statisticsexplained/>) (Accessed December 2015)
- Gelbrecht J, Lengsfeld H, Pöthig R and Opitz D 2005 Temporal and spatial variation of phosphorus input, retention and loss in a small catchment of NE Germany *J. Hydrol.* **304** 151–65
- Gu S, Gruau G, Dupas R and Jeanneau L 2020 Evidence of colloids as important phosphorus carriers in natural soil/stream waters in an agricultural catchment *J. Environ. Qual.* **49** 1–12
- Hart M R, Quin B F and Nguyen M L 2004 Phosphorus runoff from agricultural land and direct fertilizer effects: a review *J. Environ. Qual.* **33** 1954–72
- House W A and Warwick M S 1998 Intense measurement of nutrient dynamics in River Swale *Sci. Total Environ.* **210/211** 111–37
- Jensen H, Kristensen P, Jeppensen E and Skytthe A 1992 Iron:phosphorus ratio in surface sediment as an indicator of phosphate release from aerobic sediments in shallow lakes *Hydrobiologia* **253/254** 731–43
- Koopmans G F, Chardon W J, Dekker P H M, Römkens P F A M and Schoumans O F 2006 Comparing different extraction methods for estimating phosphorus solubility in various soil types *Soil Sci.* **171** 103–16
- Lee G F 1973 Role of phosphorus in eutrophication and diffuse source control *Water Res.* **7** 111–28
- Mcdonald N T, Wall D P, Mellander P E, Buckley C, Shore M, Shortle G, Leach S, Burgess E, O'Connell T and Jordan P 2019 Field scale phosphorus balances and legacy soil pressures in mixed-land use catchments *Agric. Ecosyst. Environ.* **274** 14–23
- Melland A R, Fenton O and Jordan P 2018 Effects of agricultural land management changes on surface water quality: a review of meso-scale catchment research *Environ. Sci. Policy* **84** 19–25
- Mellander P E, Jordan P, Shore M, Mcdonald N T, Wall D P, Shortle G and Daly K 2016 Identifying contrasting influences and surface water signals for specific groundwater phosphorus vulnerability *Sci. Total Environ.* **541** 292–302
- Murphy J and Riley J P 1962 A modified single solution method for the determination of phosphate in natural waters *Anal. Chim. Acta* **27** 31–36
- Rozemeijer J C and Broers H P 2007 The groundwater contribution to surface water contamination in a region with intensive agricultural land use (Noord-Brabant, The Netherlands) *Environ. Pollut.* **148** 695–706
- Rozemeijer J C and Van der Velde Y 2014 Temporal variability in groundwater and surface water quality in humid agricultural catchments; driving processes and consequences for regional water quality monitoring *Fundam. Appl. Limnol.* **184** 195–209
- Schoumans O F 2015 Phosphorous leaching from soils: process description, risk assessment and mitigation PhD Thesis (Wageningen University, Wageningen)
- Schoumans O F and Chardon W J 2014 Phosphate saturation degree and accumulation of phosphate in various soil types in The Netherlands *Geoderma* **237** 325–35
- Schoumans O F, Chardon W J, Bechmann M E, Gascuel-Odoux C, Hofman G, Kronvang B, Rubæk G H, Ulén B and Dorioz J M 2014 Mitigation options to reduce phosphorus losses

- from the agricultural sector and improve surface water quality: a review *Sci. Total Environ.* **468–469** 1255–66
- Schoumans O F and Groenendijk P 2000 Modeling soil phosphorus levels and phosphorus leaching from agricultural land in the Netherlands *J. Environ. Qual.* **29** 111–6
- Schwertmann U 1964 Differentiation of the iron oxides of the soil by extraction with ammonium oxalate solution *J. Plant Nutr. Fertilization Soil Sci.* **105** 194–202
- Smolders E, Baetens E, Verbeeck M, Nawara S, Diels J, Verdievel M, Peeters B, De Cooman W and Baken S 2017 Internal loading and redox cycling of sediment iron explain reactive phosphorus concentrations in lowland rivers *Environ. Sci. Technol.* **51** 2584–92
- Ulén B and Jakobsson C 2005 Critical evaluation of measures to mitigate phosphorus losses from agricultural land to surface waters in Sweden *Sci. Total Environ.* **344** 37–50
- Van Dael T, De Cooman T, Verbeeck M and Smolders E 2020 Sediment respiration contributes to phosphate release in lowland surface waters *Water Res.* **168** 115168
- Van der Grift B, Behrends T, Osté L A, Schot P P, Wassen M J and Griffioen J 2016a Fe hydroxyphosphate precipitation and Fe(II) oxidation kinetics upon aeration of Fe(II) and phosphate-containing synthetic and natural solutions *Geochim. Cosmochim. Acta* **186** 71–90
- Van der Grift B, Broers H P, Berendrecht W L, Rozemeijer J C, Osté L A and Griffioen J 2016b High-frequency monitoring reveals nutrient sources and transport processes in an agriculture-dominated lowland water system *Hydrol. Earth Syst. Sci. Discuss.* **12** 8337–80
- Van der Grift B, Osté L, Schot P, Kratz A, Van Popta E, Wassen M and Griffioen J 2018 Forms of phosphorus in suspended particulate matter in agriculture-dominated lowland catchments: iron as phosphorus carrier *Sci. Total Environ.* **631–632** 115–29
- Van der Grift B, Rozemeijer J C, Griffioen J and Van der Velde Y 2014 Iron oxidation kinetics and phosphate immobilization along the flow-path from groundwater into surface water *Hydrol. Earth Syst. Sci.* **18** 4687–702
- Van der Salm C, Dupas R, Grant R, Heckrath G, Iversen B V, Kronvang B, Levi C, Rubaek G H and Schoumans O F 2011 Predicting phosphorus losses with the PLEASE model on a local scale in Denmark and the Netherlands *J. Environ. Qual.* **40** 1617–26
- Withers P J A and Haygarth P M 2007 Agriculture, phosphorus and eutrophication: a European perspective *Soil Use Manage.* **23** 1–4